Am J Transl Res 2020;12(10):6136-6148
www.ajtr.org /ISSN:1943-8141/AJTR0117516

Original Article

Effect of miR-194-5p regulating STAT1/mTOR signaling pathway on the biological characteristics of ectopic endometrial cells from mice

Qian Zhao, Bing Han, Ying Zhang, Ke Su, Chunfang Wang, Panpan Hai, Aiping Bian, Ruixia Guo

Department of Gynecology, The First Affiliated Hospital of Zhengzhou University, Zhengzhou, Henan Province, China

Received July 3, 2020; Accepted August 31, 2020; Epub October 15, 2020; Published October 30, 2020

Abstract: Objective: This study aimed to find out the regulatory mechanism of miR-194-5p targeting STAT1/mTOR signaling pathway on the biological characteristics of endometrial epithelium cells from mice with endometriosis (EMs). Methods: Mouse model of EMs was constructed to observe the histopathological changes of endometrium *via* HE staining. The targeting relationship between miR-194-5p and STAT1 was verified by bioinformatics website as well as dual-luciferase reporter assay. The expressions of miR-194-5p and STAT1 in the cells were detected by qRT-PCR, then, the proliferative activity, invasion ability, apoptosis and cycle of cells were determined after overexpression of miR-194-5p, or down-regulation of miR-194-5p and STAT1. Results: In the ectopic endometrial epithelial cells, the expression of miR-194-5p was reduced, while the expression of STAT1 was significantly elevated. Overexpression of miR-194-5p or down-regulation of STAT1 significantly inhibited the proliferation and invasion and promoted apoptosis of ectopic endometrial cells. While down-regulation of miR-194-5p reversed the results, and inhibition of STAT1 partially reversed the effects partially. Conclusions: The miR-194-5p inhibits mTOR signaling pathway by inhibiting the expression of STAT1 gene, so as to inhibit the proliferation and invasion, as well as to promote the apoptosis of ectopic endometrial epithelial cells in mice with EMs.

Keywords: miR-194-5p, STAT1, mTOR signaling pathway, endometriosis

Introduction

Endometriosis (EMs) refers to a common gynecological disease in women of childbearing age, featured by endometrial cells locating in somewhere else other than the endometrium. The major pathological changes of EMs are periodic bleeding of ectopic endometrium, periodic tissue fibrosis, and formation of ectopic nodule, causing chronic pelvic pain, dysmenorrhea or infertility [1, 2]. Proliferation of ectopic endometrial cells has been confirmed to be an important factor for the angiogenesis and persistence of ectopic lesions [3]. The pathogenesis of EMs involves the regulation of a variety of cytokines, and the coordination and transduction of multiple signaling pathways [4]. Therefore, it is of great significance to find out the regulatory factors and pathways involved in the pathogenesis of EMs.

Signal transducer and activator of transcription 1 (STAT1) is widely expressed in various tissues and cells, and dimers from STAT1 (autophosphorylation) can go into the nucleus, and regulate the cell cycle, vascular endothelial factor, and proliferative or apoptosis-related factors [5]. Expression of STAT3 was significantly enhanced, and the mTOR pathway was activated in patients with meningioma, according to Johnson [6]. Furthermore, the excessive activation of STAT3 was also found in patients with EMs, which may relate to the dysregulation of decidualization of ectopic endometrial cells [7]. Both STAT1 and STAT3 are important members of the STAT family, but whether STAT1 affects the pathogenesis of EMs is not clear yet.

MiRNAs are a class of non-coding micro RNA with a length of about 22 bases, which could participate in the pathogenesis of EMs, including hypoxia, inflammatory response, neovascularization, apoptosis and tissue repair [8]. There were various miRNAs expressing differently in the endometrial tissues of patients with EMs and infertility, which may relate to the patho-

genesis of EMs [9]. Through bioinformatics software, we found that STAT1 and miR-194-5p had targeted binding sites. The miR-194 is one of the non-coding miRNAs, and miR-194-3p has been found to participate in the pathogenesis of EMs by regulating the expression of progesterone receptors and decidualization [10]. The 5'UTR segment of miRNA has been proved to have the same function of inhibiting target miRNAs as the 3'UTR segment does [11]. Therefore, we speculated that miR-194-5p may target STAT1 and affect the progress of EMs.

In the present study, from the perspective of biological characteristics of ectopic endometrial cells on the pathogenesis of EMs, the targeting relationship between miR-194-5p and STAT1 was confirmed by reviewing the predecessor literature and analyzing website. We aimed to find out the specific mechanism of miR-194-5p and STAT1 on regulating the biological characteristics of ectopic endometrial cells and participating the pathogenesis of EMs.

Materials and methods

Construction of mouse model

A total of 45 clean inbred BALB/c female mice, 4-5 weeks old, weighing 20-25 g, were purchased from the Experimental Animal Center of Guangzhou University of Chinese Medicine. With the use of a random method, 15 mice with two consecutive normal estrous cycles were selected from the 45 mice to construct mouse models of EMs (Model group), and 15 mice with two consecutive normal estrous cycles were included in the Normal group, and the other 15 in the Sham group (sham-operated group). The construction of mouse model was referenced to literature about EMs [12]. In the third period of estrus, the mice were anesthetized, and ligated at the left side of the uterus with the use of No. 5 suture. Then, 3 pieces of 2*2 mm were removed from the isolated uterus of the mouse by a biopsy punch, and sutured on the mesenterium with well-perfused blood vessels. After the operation, we kept the mice warm, let them wake up naturally, and kept them clean. All mice were intramuscularly injected with gentamicin to prevent infection (for 3 consecutive days). In the Sham group, same size of omental fat was used as the graft, and the rest of the measures were the same as the Model group. In the Normal group, mice received no treatment. Four weeks after construction, the ectopic endometrial growth of the model mice was observed after laparotomy. The successful EMs model was characterized by increased volume of the graft, neovascularization on the graft surface, and small sacs containing transparent liquid on the graft [13]. Two mice died during modeling, and the remaining mice were successfully modeled, with a success rate of 86.67%. All of the above experiment was approved by the Animal Care and Use Committee of The First Affiliated Hospital of Zhengzhou University (No. ZZU20190316).

Sample acquisition

After successful modeling, all mice were sacrificed by decapitation. The abdominal cavity was opened layer by layer on the aseptic operation table, and the endometrial tissues were harvested. A part of tissues was immediately fixed with 4% paraformaldehyde solution, embedded in paraffin, and serially sliced in a thickness of 4 μm. Other tissues were placed in liquid nitrogen and then stored at -80°C for later use.

HE staining

Paraffin sections were dewaxed twice with xylene, 5 minutes for each time, then dehydrated with 100%, 95%, 80%, and 75% ethanol for 1 min, respectively, rinsed with tap water for 2 min, stained with hematoxylin for 2 min, and rinsed with tap water for another 10 s. Next, the sections were differentiated and washed with 1% hydrochloric acid alcohol, immersed in 1% ammonium hydroxide for 30 s, washed in distilled water for 1 min, stained with eosin for 2 min, and again washed in distilled water for 10 s. Then, the slices were dehydrated twice with 95% and 100% ethanol, respectively, 1 min for each time. After dewaxed with xylene, the slices were sealed with neutral gum. Finally, the sections were observed under a 400-fold ordinary light microscope for the pathological morphology of the ectopic lesions.

Dual-luciferase reporter assay

Target gene analysis of miR-194-5p was performed with biological prediction site, targetscan.org. Besides, dual-luciferase reporter assay was conducted to verify whether STAT1 is

Table 1. Primer sequence

Name	Primer sequence (5'-3')
miR-194-5p	F: TCGACTGAAGCATAGCTGACAG
	R: AGTCTCGACTAACAGTCAGTAC
STAT1	F: AGA CCA CCT CTC TTC CTG TCGT
	R: AAA CTGCCA ACT CAA CAC CTCT
mTOR	F: ATGCTTGGAACCGGACCTG
	R: TCTTGACTCATCTCTCGGAGTT
Cyclin D1	F: TGGAGCCCCTGAAGAAGAG
	R: AAGTGCGTTGTGCGGTAGC
MMP-2	F: CTATTCTGCCAGCACTTTGG
	R: CAGACTTTGGTTCTCCAACTT
MMP-9	F: ACGGCAACGGAGAAGGCAAACC
	R: AGACGAAGGGGAAGACGCACAGC
Bax	F: AGCTGCAGAGGATGATTGCT
	R: CTGATCAGCTCGGGCACTTTA
Bcl-2	F: GCCTCCTCACCTTTCAGCAT
	R: CACTCGTAGCCCTCTGTGAC
U6	F: GCTTCGGCAGCACATATACTAAAAT
	R: CGCTTCACGAATTTGCGTGTCAT
GAPDH	F: CACGGCAAGTTCAACGGCACAGTCA
	R: GTGAAGACGCCAGTAGACTCCACGAC

a direct target gene of miR-194-5p. The 3'UTR segment of the STAT1 gene was cloned and amplified, and the PCR product was cloned into the downstream polyclonal site of pmirGLO (Promega, USA) Luciferase gene, named pSTAT1-Wt. Then, the binding site of miR-194-5p and the target gene was predicted, specific to bioinformatics, for site-directed mutagenesis, and construction of pSTAT1-Mut vector. The pRL-and TK vector (Promega, USA) expressing Renilla luciferase was an internal reference to adjust the difference in cell number and transfection efficiency. The miR-194-5p mimic and the negative control were co-transfected into ectopic endometrial epithelial cells with luciferase reporter vector, respectively, and the dual-luciferase reporter assay was performed according to the instruction provided by Promega.

Culture, transfection and grouping of endometrial epithelium cells

The ectopic endometrial cells and normal endometrial cells near the ectopic endometrium in the Model group were extracted, cut into tissue pieces in about 3 mm^3, washed twice with PBS, inoculated in DMEM (Gibco, USA) containing 10% fetal bovine serum (FBS, Excell Bio, Shanghai, China), and cultured in a 5% CO_2 incubator at 37°C. After a large number of epithelial cells were exfoliated, the solution was changed every 3 days. The culture medium was discarded after 80%-90% cell fusion. The cells were then washed twice with PBS, digested with 0.25% trypsin, adjusted to a concentration of $1.0*10^6$ cells/mL in DMEM containing 10% FBS, and seeded into the culture plate and petri dish for continuous culture. The cells were divided into 7 groups: Control group (normal endometrial cells), and other 6 groups of ectopic endometrial cells: Blank group (no transfection), NC group (transfected with miR-194-5p negative control sequence), miR-194-5p mimic group (with miR-194-5p mimic), miR-194-5p inhibitor group (with miR-194-5p inhibitor), siRNA-STAT1 group (with siRNA-STAT1), and miR-194-5p inhibitor + siRNA-STAT1 group (with miR-194-5p inhibitor and siRNA-STAT1). All the transfection plasmids were purchased from Sangon Biotech, Shanghai, China.

Cells in logarithmic growth phase were seeded in 96-well plates to a cell density of 50%. Transfection were performed according to the instructions of Lipofectamine 2000 (Invitrogen, USA). First, 250 μL of serum-free Opti-MEM (Gibco, USA) was used for diluting 100 pmol of miR-194-5p mimic, miR-194-5p inhibitor, siRNA-STAT1, miR-194-5p inhibitor + siRNA-STAT1, and negative control, respectively, and then incubated for 5 min at room temperature. Second, 250 μL of serum-free Opti-MEM was used for diluting 5 μL of lipofectamine 2000, also incubated for 5 min at room temperature. Third, the above two were mixed, incubated for 20 min at room temperature, added in the cell culture wells, and cultured in 5% CO_2 incubator at 37°C for 6-8 hours. Last, the medium was replaced by complete medium, and the cells were cultured for another 48 h before subsequent experiments.

qRT-PCR

Total RNA was extracted from the transfected cells using Trizol kit (Invitrogen, USA). Primer 5 software was applied to design miR-194-5p, STAT1, mTOR, cyclinD1, MMP-2, MMP-9, Bax, Bcl-2 primers (**Table 1**). RNA template, Primer Mix, dNTP Mix, DTT, RT Buffer, HiFi-MMLV and RNase-free water were dissolved on ice for use. Reverse transcription system was in a volume of 20 μL, performed according to the instruc-

tions of TaqMan MicroRNA Assays Reverse Transcription Primer (Thermo scientific, USA). The reaction conditions were set at 42°C for 30-50 min (reverse transcription reaction), 85°C for 5 s (inactivation of reverse transcriptase enzyme). The reaction solution was subjected to quantitative PCR. The 50 μL reaction system included 25 μL of SYBR® Premix Ex Taq™ II (2×), 2 μL of PCR forward primers, 2 μL of PCR reverse primers, 1 μL of ROX Reference Dye (50×), 4 μL of DNA template, and 16 μL of ddH_2O.

Western blot

The transfected cells were collected, and extracted for total protein. The protein concentration was determined by BCA kit (Abeam, UK). The protein was quantified according to concentrations, separated by polyacrylamide gel electrophoresis, transferred to PVDF membrane, and sealed with 5% BSA at room temperature for 1 h. Dilute primary antibodies (rabbit anti-mouse) were all from Abcam, UK, included STAT1 (ab109320, 1/1,000), p-STAT1 (ab30645, 1/1,000), p-mTOR (ab109268, 1/1,000), cyclinD1 (ab40754, 1/1,000), MMP-2 (ab37150, 1/1,000), MMP-9 (ab38898, 1/1,000), Bax (ab32503, 1/1,000), Bcl-2 (ab692, 1/1,000), and GAPDH (ab181602, 1/5,000) were instilled and incubated over night at 4°C on a shaker. The membrane was washed 3 times of 5 min with TBST. Then, horseradish peroxidase-labeled goat anti-rabbit IgG (ab6721, 1/2,000, Abcam, UK) dilution was added and incubated for 1 h at room temperature. The membrane was again washed (same as above). ECL reagent (Pierce, USA) was added prior to protein quantitative analysis (ImageJ software).

MTT assay

The transfected cells were collected and prepared as cell suspension of $3*10^3$-$5*10^3$ cells/mL with the use of RPMI 1640 medium containing 10% FBS, and seeded into 96-well tissue culture plates. Six duplicate wells were prepared for each experiment group, with 100 μL per well. The cells were then cultured in a 5% CO_2 incubator at 37°C. Each well was added with 20 μL of 5 mg/mL MTT solution (Gibco, USA) at the 24th h, 48th h, and 72th h, then continuously incubated at 37°C for another 4 h. After that, and the culture supernatant in the wells was discarded. The optical density value of each well was measured with an automatic microplate reader at 570 nm (BIO-RAD, USA).

Transwell

First, 200 μL of cells were seeded in the Transwell chamber, and 600 μL of RPMI 1640 medium containing 20% FBS (Gibco, USA) was added in the plate. Second, the cells were placed in an incubator at 37°C for 24 h of incubation. Third, cells on the internal surface of chamber were wiped with cotton swabs, and the chamber was rinsed with PBS for 3 min, immersed with formaldehyde for 10 min, then washed with water for 3 times of 3 min. Next, the cells were stained for 15 min with 0.5% crystal violet solution (Solarbio, Beijing, China), then washed with PBS for 3 times. Last, 5 fields of view were randomly selected and photographed with an inverted microscope for cell counting.

Flow cytometry

The cell cycle was detected as follows. The transfected cells of each group were digested with 0.25% trypsin (Thermo, USA), adjusted to a concentration of $1*10^5$ cells/mL, fixed with -20°C pre-cooled ethanol solution with a volume fraction of 75%, and placed at 4°C overnight. Next, 1 mL of cells was centrifuged at 1,500 r/min for 5 min, and washed twice with PBS after the discard of cooled ethanol. Then, the supernatant was removed, and the cell suspension was added with 1 mL of 50 mg/L propidium iodide (containing RNase) (Sigma, USA), and placed in dark for 30 minutes at 4°C. Last, the red fluorescence was detected by flow cytometry (Beckman Coulter, USA) at an excitation wavelength of 488 nm.

The apoptosis detection procedures were the as the detection of cell cycle until centrifugation. After that, the cells were washed twice with PBS, resuspended in 200 μL binding buffer by centrifugation, added with 5 μL of Annexin V-FITC and 10 μL of propidium iodide (Sigma, USA), gently mixed, placed in dark for 15 min at room temperature, and then added with 300 μL HEPES buffer. Annexin V-FITC fluorescence signal was detected at an excitation wavelength of 488 nm and 530 nm, and propidium iodide fluorescence signal was detected at an excitation wavelength of over 575 nm by flow cytometry (Beckman Coulter, USA).

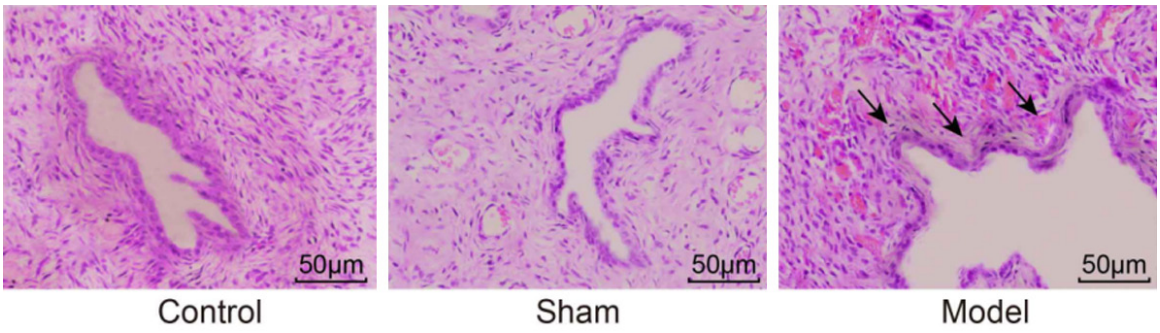

Figure 1. Pathological changes of endometrial tissues in each group (200×). Results of HE showed well growth of the endometrial epithelial cells in the control group and the Sham group, with large and pleated glandular cavity. In the Model group, the endometrial lesions of the mice were polycystic, with obvious congestion and decrescent glandular cavity, showing cell pyknosis and deep staining of cytoplasm (indicated by arrows).

Statistical analysis

Data were processed by SPSS 21.0. The quantitative data were expressed as mean ± standard deviation, compared among multiple groups by one-way analysis of variance, and compared between any two groups by post-hoc Bonferroni test. $P<0.05$ was considered statistically prominent.

Results

Pathological changes of endometrial tissues

Two mice died during the modeling process, and the remaining mice were successfully modeled with a success rate of 86.67%. Results of HE showed well growth of the endometrial epithelial cells in the Normal group and the Sham group, with large and pleated glandular cavity. In the Model group, the endometrial lesions of the mice were polycystic, with obvious congestion and decrescent glandular cavity, showing cell pyknosis and deep staining of cytoplasm. See **Figure 1**.

Targeted regulation of mir-194-5p on STAT1

Gene analysis of miR-194-5p was carried out using the predicted website http://www.targetscan.org/vert_72/, and the binding sites of miR-194-5p to STAT1 are shown in **Figure 2A**.

We applied the dual-luciferase assay to verify the targeting relationship between miR-194-5p and STAT1. The co-transfected NC mimic and STAT1-WT plasmids had declined luciferase activity as compared with co-transfection of miR-194-5p mimic and STAT-WT plasmids ($P<0.05$). See **Figure 2B**.

The mRNA and protein levels of STAT1 changed when miR-194-5p was overexpressed or inhibited (**Figure 3**). Compared with the Control group, the remaining groups showed decreased expression of miR-194-5p, and elevated levels of STAT1 and p-STAT1 (all $P<0.05$). There was no significant difference between Blank and NC groups.

Compared with Blank group, miR-194-5p mimic group had elevated expression of miR-194-5p, and reduced mRNA and protein expressions of STAT1 were (all $P<0.05$); siRNA-STAT1 group presented no significant difference in the level of miR-194-5p, but showed reduced levels of STAT1 and p-STAT1 (both $P<0.05$); miR-194-5p inhibitor group had declined level of miR-194-5p, and elevated levels of STAT1 and p-STAT1 (all $P<0.05$); miR-194-5p inhibitor + siRNA-STAT1 group had declined level of miR-194-5p ($P<0.05$), and presented no significant difference in levels of STAT1 and p-STAT1 (both $P>0.05$).

The above experiments demonstrated that miR-194-5p negatively regulated the expression of STAT1.

Protein and mRNA levels of mTOR, cyclinD1, MMP-2, MMP-9, Bax and Bcl-2 after transfection (qRT-PCR and western blot)

Detection of mTOR signaling factors showed that compared with the Control group, the levels of mTOR mRNA, and p-mTOR protein were elevated in the remaining groups; the miR-194-5p mimic group and siRNA-STAT1 group showed opposite results as compared with Blank group; miR-194-5p inhibitor group had elevated

A

	Predicted consequential pairing of target region (top) and miRNA (bottom)	Site type
Position 1248-1254 of STAT1 3' UTR	5' . . . AAAAAGAACUUUCAGCUGUUACU. . .	7mer-m8
mmu-miR-194-5p	3' AGGUGUACCUCAACGACAAUGU	

B

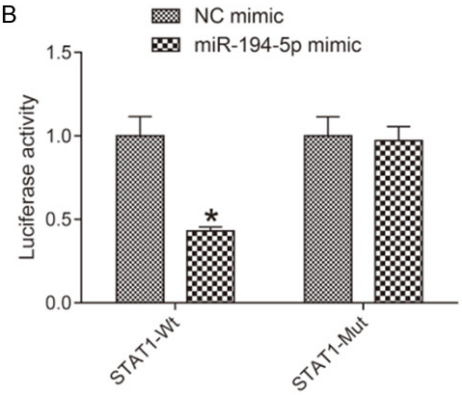

Figure 2. Targeted regulation of miR-194-5p on STAT1. A. The sequence of the 3'UTR segment of miR-194-5p binding to STAT1; B. Luciferase activity detected by dual luciferase assay. Compared with the NC mimic group, *P<0.05.

expressions of mTOR mRNA and p-mTOR protein as compared with the Blank group (all P<0.05).

Detection factors related to invasion and metastasis showed that compared with the Control group, the mRNA and protein expressions of cyclinD1, MMP-2, MMP-9 were elevated (all P<0.05). Compared with Blank group, miR-194-5p inhibitor group had showed similar results, while the miR-194-5p mimic group and siRNA-STAT1 group had the opposite (all P<0.05).

Detection of apoptosis-related factor showed that compared with Control group, the mRNA and protein levels of Bcl-2 were elevated, while of Bax were reduced (all P<0.05). Compared with Blank group, miR-194-5p inhibitor group presented similar results, while the miR-194-5p mimic group and siRNA-STAT1 group had the opposite (all P<0.05). See **Figure 4**.

Proliferation activity of cells after transfection

Compared with Control group, the cell proliferation activity of the other groups was elevated (all P<0.05). Compared with the Blank group, the activity in miR-194-5p mimic and siRNA-STAT1 groups was reduced, and in miR-194-5p inhibitor group was elevated (all P<0.05), while there were no significant difference presented in NC and the miR-194-5p inhibitor + siRNA-STAT1 groups. The difference in cell proliferation between miR-194-5p mimic and siRNA-STAT1 groups was also not significant. See **Figure 5**.

Invasion ability of cells after transfection

Compared with Control group, the invasion ability of the other groups was elevated (all P<0.05). Compared with the Blank group, the cell invasion ability in miR-194-5p mimic and siRNA-STAT1 groups was reduced, and inmiR-194-5p inhibitor group was elevated (all P<0.05), while there were no significant difference presented in NC and miR-194-5p inhibitor + siRNA-STAT1 groups. The difference in cell invasion ability between miR-194-5p mimic group and siRNA-STAT1 group was also not significant. See **Figure 6**.

Apoptosis and cell cycle after transfection

Compared with Control group, the apoptosis rate of the other groups was reduced (all P<0.05). Compared with the Blank group, the apoptosis rate in miR-194-5p mimic and siRNA-STAT1 groups was elevated, and in miR-194-5p inhibitor group was reduced (all P<0.05), while there were no significant difference presented in NC and miR-194-5p inhibitor + siRNA-STAT1 groups. The difference in apoptosis rate between miR-194-5p mimic and siRNA-STAT1 groups also not significant. See **Figure 7**.

Compared with Control group, the proportion of cells in the G0/G1 phase of the other groups was reduced, while that in S phase was promi-

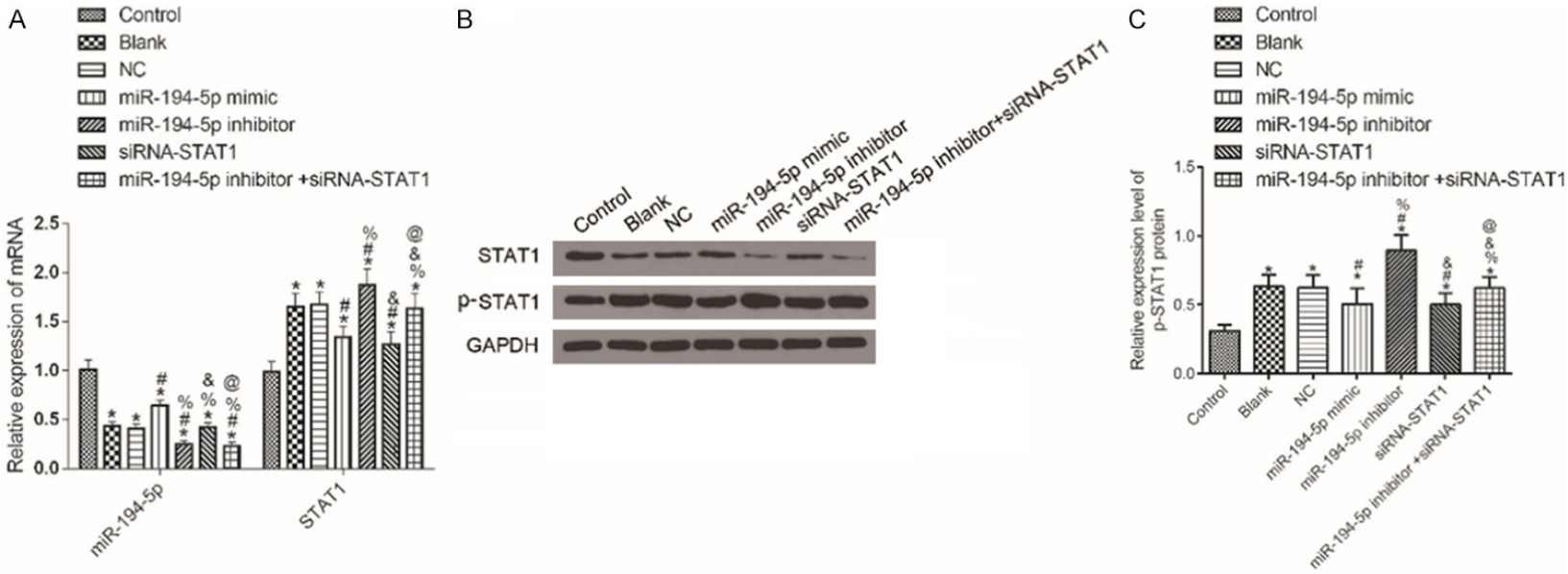

Figure 3. Expression of miR-194-5p on STAT1 in endometrial cells from mice. A. Expression of mRNA; B. Protein bands; C. Quantification of protein expressions. Compared with the Control group, $^{*}P<0.05$; compared with the Blank group, $^{\#}P<0.05$; compared with the miR-194-5p mimic group, $^{\%}P<0.05$; compared with the miR-194-5p inhibitor group, $^{\&}P<0.05$; compared with the siRNA-STAT1 group, $^{@}P<0.05$.

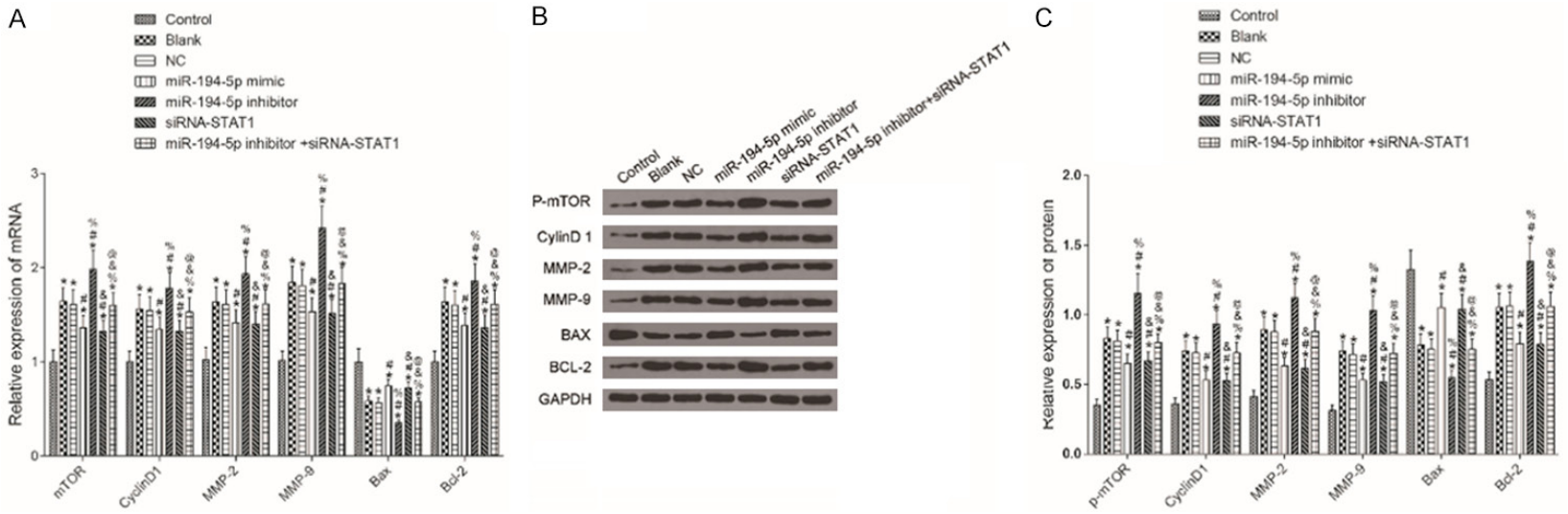

Figure 4. Protein and mRNA expression levels of mTOR, cyclinD1, MMP-2, MMP-9, Bax and Bcl-2. A. Expression of mRNA; B. Protein bands; C. Quantification of protein expression. Compared with the Control group, $^{*}P<0.05$; compared with the Blank group, $^{\#}P<0.05$; compared with the miR-194-5p mimic group, $^{\%}P<0.05$; compared with the miR-194-5p inhibitor group, $^{\&}P<0.05$; compared with the siRNA-STAT1 group, $^{@}P<0.05$.

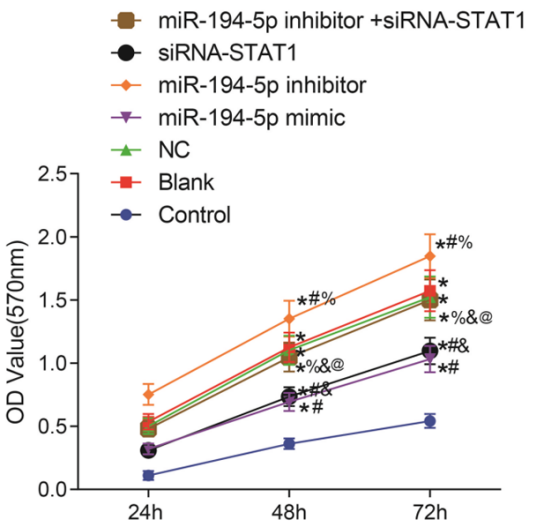

Figure 5. Proliferation of cells after transfection. Compared with the Control group, *P<0.05; compared with the Blank group, #P<0.05; compared with the miR-194-5p mimic group, %P<0.05; compared with the miR-194-5p inhibitor group, &P<0.05; compared with the siRNA-STAT1 group, @P<0.05.

nently increased (all P<0.05). Compared with the Blank group, the proportion in the G0/G1 phase was elevated, and in S phase was reduced in miR-194-5p mimic and siRNA-STAT1 groups (all P<0.05); the miR-194-5p inhibitor group had the opposite results (both P<0.05), but no significant difference in NC and miR-194-5p inhibitor + siRNA-STAT1 groups. The difference in cell cycle ratio between the miR-194-5p mimic group and siRNA-STAT1 group was also not significant. The differences in cells in the G2 phase among each group were not significant. See **Figure 8**.

Discussion

The development of EMs is the result of a combination of immune, estrogen, genetic, vascular and other factors [14, 15]. Epigenetic disorders caused by differential expression of miRNA may be associated with the pathogenesis of EMs [6]. In this study, we constructed mouse model of EMs and studied miRNA regulating genes and pathways that influence the pathogenesis of EMs. The results confirmed that miR-194-5p can inhibit the expression of STAT1 gene, promote the activation of mTOR pathway, and thus inhibit the proliferation and invasion of ectopic endometrial epithelial cells in mice with EMs.

It has been reported that miRNAs affect the pathogenesis of EMs. For example, Nematian et al. reported that patients with EMs had elevated miR-125b-5p expression and decreased miR-7b-5p expression in serum, and both miR-125b-5p and miR-7b-5p played a regulatory role in the production of proinflammatory cells of EMs [16]. In addition, down-regulation of miR-183 can inhibit the apoptosis of endometrial stromal cells and promote proliferation and invasion of cells in patients with EMs [17]. This study further found that the expression of miR-194-5p was decreased; expression of STAT1 was increased in mouse model of EMs compared to the Control group. The STAT family is mainly composed of transcription factors, with a total of 7 members [18]. Currently, STAT3 is extensively studied, and numerous studies have confirmed that STAT3 activation is involved in cell proliferation and neovascularization, and plays an important role in the pathogenesis of EMs [19, 20]. Besides, enhanced expression of miR-210 can activate STAT3 and promote the pathogenesis of EMs [21]. Based on previous studies, this study further confirmed that STAT1, an important member of the STATS family, was significantly activated in ectopic lesions of EMs mice.

The mTOR pathway is important in promoting cell proliferation and neovascularization [22-24]. Study found that the proliferation of ectopic endometrial cells was increased in patients with EMs, and was associated with over-activation of the mTOR pathway, while mTOR signaling pathway inhibitors were effective in inhibiting the proliferation of ectopic endometrial cells [25]. Additionally, the activation of mTOR in lesions of EMs can promote the increase of Bcl-2/Bax ratio, and inhibit autophagy and apoptosis of endometrial cells [26]. This study also found that the mTOR pathway was activated in EMs mice, and overexpression of miR-194-5p or silencing of STAT1 can inhibit mTOR expression. MMP-2 and MMP-9 are proteolytic enzymes that play important roles in organisms, and are involved in the invasion and metastasis of various tumor cells [27, 28]. In recent years, increasing studies have confirmed that the enhancement of MMP-2 and MMP-9 expression is closely related to the invasion and metastasis of EMs [29, 30]. This study found that compared with the Control group, the expressions of cyclinD1, MMP-2, MMP-9

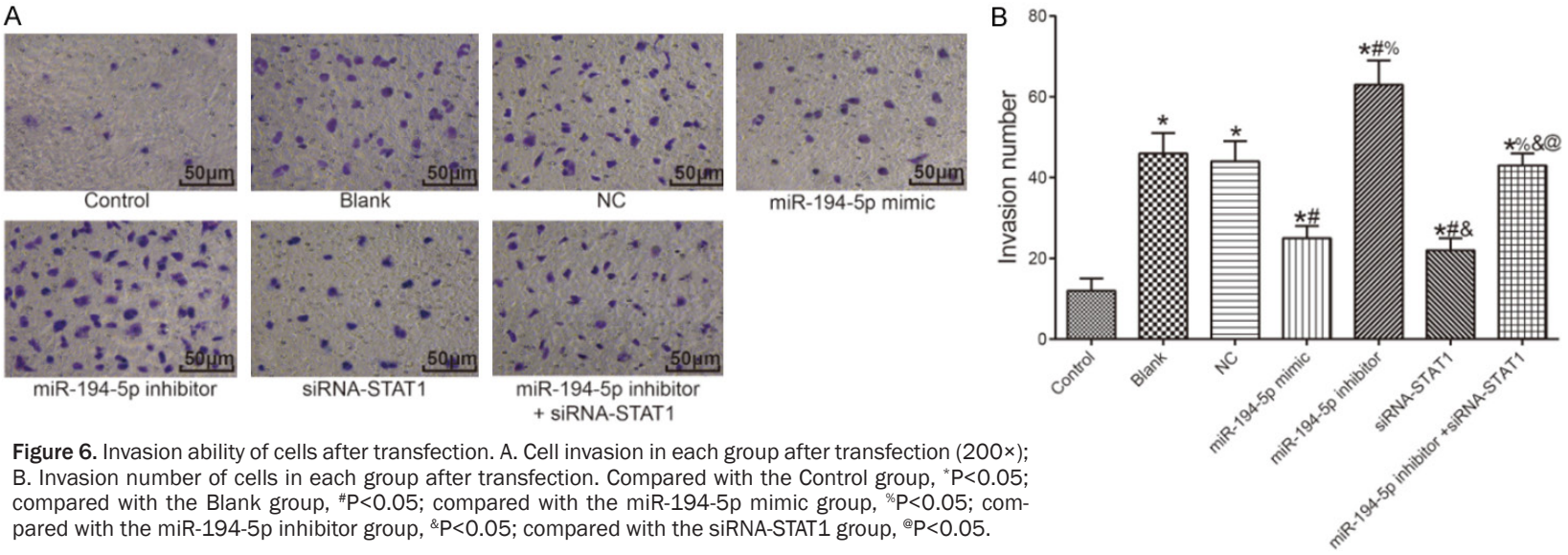

Figure 6. Invasion ability of cells after transfection. A. Cell invasion in each group after transfection (200×); B. Invasion number of cells in each group after transfection. Compared with the Control group, $^{*}P<0.05$; compared with the Blank group, $^{\#}P<0.05$; compared with the miR-194-5p mimic group, $^{\%}P<0.05$; compared with the miR-194-5p inhibitor group, $^{\&}P<0.05$; compared with the siRNA-STAT1 group, $^{@}P<0.05$.

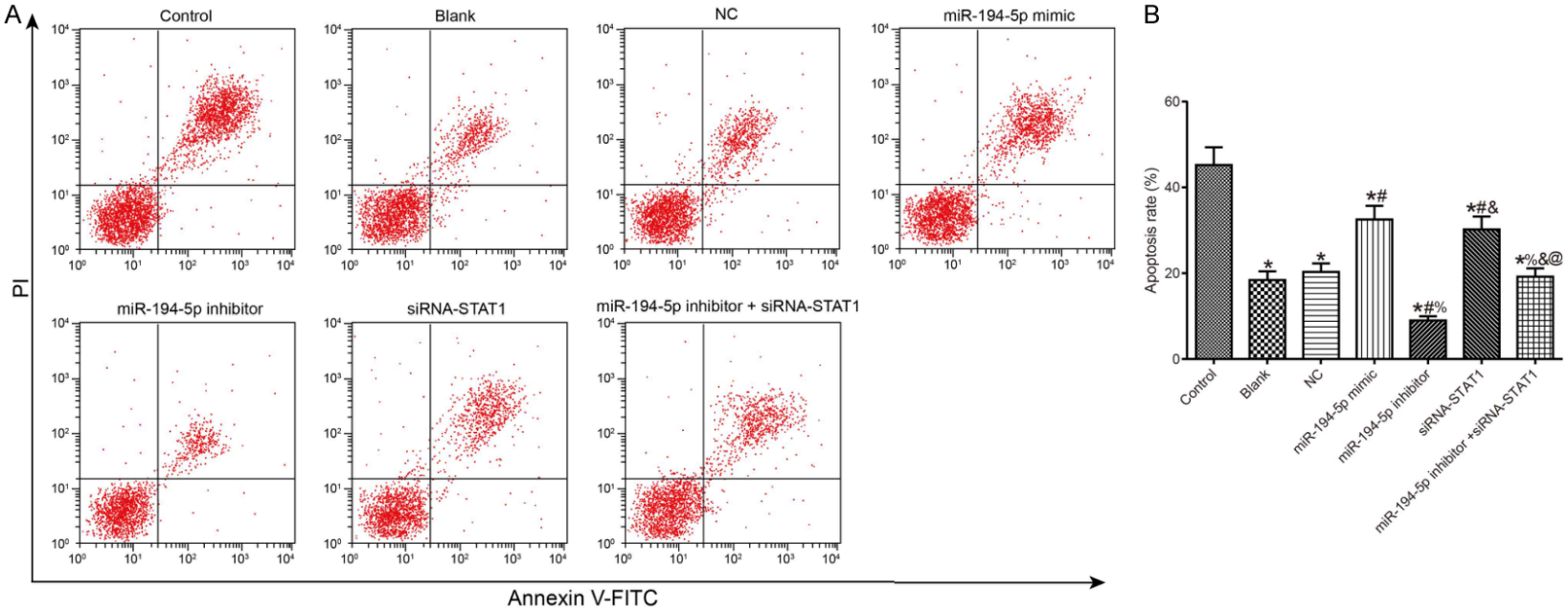

Figure 7. Apoptosis after transfection detected by flow cytometry. A. Apoptosis of each group after transfection; B. Apoptosis rate of each group after transfection. Compared with the Control group, *P<0.05; compared with the Blank group, #P<0.05; compared with the miR-194-5p mimic group, %P<0.05; compared with the miR-194-5p inhibitor group, &P<0.05; compared with the siRNA-STAT1 group, @P<0.05.

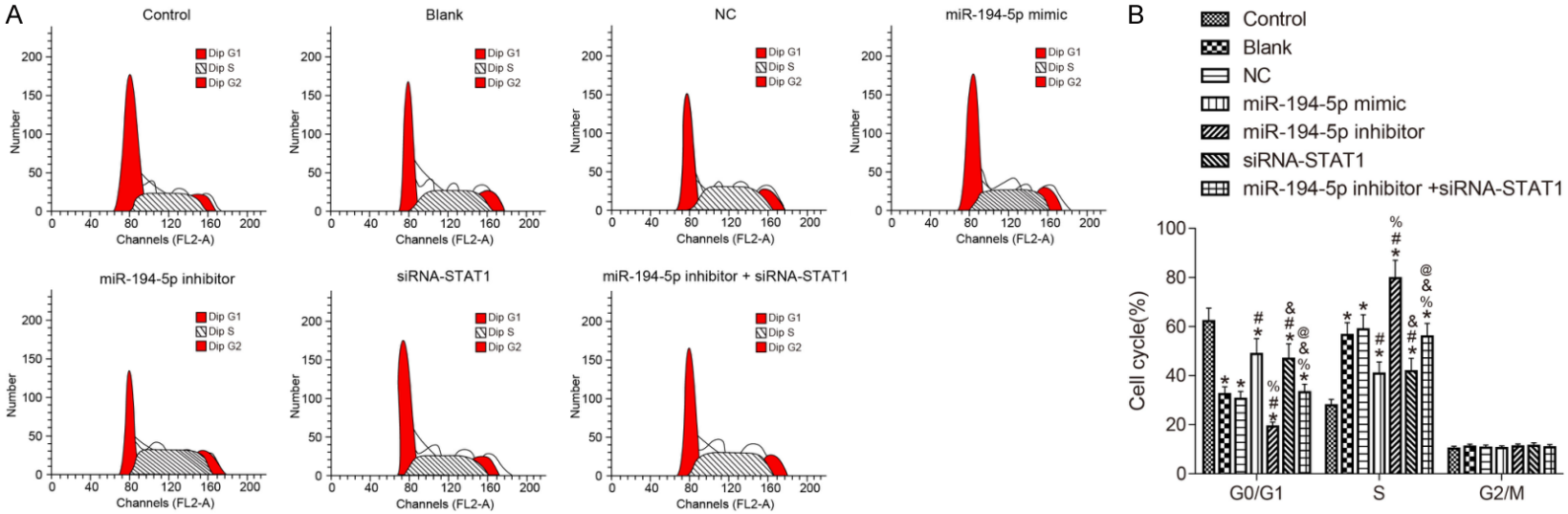

Figure 8. Cell cycle after transfection detected by flow cytometry. A. Cell cycle of each group after transfection; B. Proportion of cell cycle in each group after transfection. Compared with the Control group, *P<0.05; compared with the Blank group, #P<0.05; compared with the miR-194-5p mimic group, %P<0.05; compared with the miR-194-5p inhibitor group, &P<0.05; compared with the siRNA-STAT1 group, @P<0.05.

and pro-apoptotic protein Bcl-2 in the ectopic endometrial cells of EMs mice were enhanced, while the expression of anti-apoptosis protein Bax was reduced. Overexpression of miR-194-5p or inhibition of STAT1 can reverse the above changes. Moreover, MTT and Transwell experiments showed that overexpression of miR-194-5p or silencing of STAT1 can inhibit invasion and viability of ectopic endometrial cells, while miR-194-5p inhibitor can counteract the effect of STAT1 silencing on ectopic endometrial cells. The results of flow cytometry showed that the apoptosis of the miR-194-5p overexpression group and the siRNA-STAT1 group were increased compared with Blank and NC groups, and more cells were retarded in the G0/G1 phase, suggesting that overexpression of miR-194-5p can inhibit STAT1 and promote apoptosis.

In this study, we investigated the effects of miR-194-5p regulating STAT1/mTOR pathway on the biological characteristics of ectopic endometrial cells from the perspective of molecular mechanism of pathogenesis in mouse model of EMs, but other aspects of EMs such as ectopic endometrial adhesion were not explored, and corresponding *in vitro* tissue and animal experiments were not carried out because of the limitation of time and research grant. So, further study of this topic will be performed in the future. In conclusion, miR-194-5p can targetedly inhibit the STAT1 gene, the mTOR signaling pathway, the proliferation and invasion of ectopic endometrial cells in EMs mice, as well as promote cell apoptosis.

Disclosure of conflict of interest

None.

Address correspondence to: Ruixia Guo, Department of Gynecology, The First Affiliated Hospital of Zhengzhou University, No. 1 Jianshe East Road, Zhengzhou 450052, Henan Province, China. Tel: +86-0371-67966021; E-mail: guoruixia7k9@163.com

References

[1] Vercellini P, Somigliana E, Vigano P, Abbiati A, Barbara G and Crosignani PG. Endometriosis: current therapies and new pharmacological developments. Drugs 2009; 69: 649-675.

[2] Berlac JF, Hartwell D, Skovlund CW, Langhoff-Roos J and Lidegaard O. Endometriosis increases the risk of obstetrical and neonatal complications. Acta Obstet Gynecol Scand 2017; 96: 751-760.

[3] Tsai HW, Huang MT, Wang PH, Huang BS, Chen YJ and Hsieh SL. Decoy receptor 3 promotes cell adhesion and enhances endometriosis development. J Pathol 2018; 244: 189-202.

[4] Hou XX, Zhou WJ, Wang XQ and Li DJ. Fractalkine/CX3CR1 is involved in the pathogenesis of endometriosis by regulating endometrial stromal cell proliferation and invasion. Am J Reprod Immunol 2016; 76: 318-325.

[5] Chung SS, Adekoya D, Enenmoh I, Clarke O, Wang P, Sarkyssian M, Wu Y and Vadgama JV. Salinomycin abolished STAT3 and STAT1 interactions and reduced telomerase activity in colorectal cancer cells. Anticancer Res 2017; 37: 445-453.

[6] Johnson MD, O'Connell M, Vito F and Bakos RS. Increased STAT-3 and synchronous activation of Raf-1-MEK-1-MAPK, and phosphatidylinositol 3-Kinase-Akt-mTOR pathways in atypical and anaplastic meningiomas. J Neurooncol 2009; 92: 129-136.

[7] Dimitriadis E, Sharkey AM, Tan YL, Salamonsen LA and Sherwin JR. Immunolocalisation of phosphorylated STAT3, interleukin 11 and leukaemia inhibitory factor in endometrium of women with unexplained infertility during the implantation window. Reprod Biol Endocrinol 2007; 5: 44.

[8] Saare M, Rekker K, Laisk-Podar T, Rahmioglu N, Zondervan K, Salumets A, Götte M and Peters M. Challenges in endometriosis miRNA studies - from tissue heterogeneity to disease specific miRNAs. Biochim Biophys Acta Mol Basis Dis 2017; 1863: 2282-2292.

[9] Haikalis ME, Wessels JM, Leyland NA, Agarwal SK and Foster WG. MicroRNA expression pattern differs depending on endometriosis lesion type. Biol Reprod 2018; 98: 623-633.

[10] Pei T, Liu C, Liu T, Xiao L, Luo B, Tan J, Li X, Zhou G, Duan C and Huang W. miR-194-3p represses the progesterone receptor and decidualization in eutopic endometrium from women with endometriosis. Endocrinology 2018; 159: 2554-2562.

[11] Lytle JR, Yario TA and Steitz JA. Target mRNAs are repressed as efficiently by microRNA-binding sites in the 5'UTR as in the 3'UTR. Proc Natl Acad Sci U S A 2007; 104: 9667-9672.

[12] Alvarez P, Bogen O, Chen X, Giudice LC and Levine JD. Ectopic endometrium-derived leptin produces estrogen-dependent chronic pain in a rat model of endometriosis. Neuroscience 2014; 258: 111-120.

[13] Sharpe-Timms KL. Using rats as a research model for the study of endometriosis. Ann N Y Acad Sci 2002; 955: 318-327; discussion 340-312, 396-406.

[14] Dodds KN, Beckett EAH, Evans SF and Hutchinson MR. Lesion development is modulated by the natural estrous cycle and mouse strain in a minimally invasive model of endometriosis. Biol Reprod 2017; 97: 810-821.
[15] Takeuchi K and Satoh H. NSAID-induced small intestinal damage--roles of various pathogenic factors. Digestion 2015; 91: 218-232.
[16] Nematian SE, Mamillapalli R, Kadakia TS, Majidi Zolbin M, Moustafa S and Taylor HS. Systemic inflammation induced by microRNAs: endometriosis-derived alterations in circulating microRNA 125b-5p and Let-7b-5p regulate macrophage cytokine production. J Clin Endocrinol Metab 2018; 103: 64-74.
[17] Shi XY, Gu L, Chen J, Guo XR and Shi YL. Downregulation of miR-183 inhibits apoptosis and enhances the invasive potential of endometrial stromal cells in endometriosis. Int J Mol Med 2014; 33: 59-67.
[18] Zhang Y, Jin G, Zhang J, Mi R, Zhou Y, Fan W, Cheng S, Song W, Zhang B, Ma M and Liu F. Overexpression of STAT1 suppresses angiogenesis under hypoxia by regulating VEGFA in human glioma cells. Biomed Pharmacother 2018; 104: 566-575.
[19] Kim BG, Yoo JY, Kim TH, Shin JH, Langenheim JF, Ferguson SD, Fazleabas AT, Young SL, Lessey BA and Jeong JW. Aberrant activation of signal transducer and activator of transcription-3 (STAT3) signaling in endometriosis. Hum Reprod 2015; 30: 1069-1078.
[20] Okamoto M, Nasu K, Kai K, Aoyagi Y, Hirakawa T and Narahara H. The effects of STAT3 inhibitors on endometriotic cyst stromal cells. J Reprod Immunol 2015; 112: 138-138.
[21] Okamoto M, Nasu K, Abe W, Aoyagi Y, Kawano Y, Kai K, Moriyama M and Narahara H. Enhanced miR-210 expression promotes the pathogenesis of endometriosis through activation of signal transducer and activator of transcription 3. Hum Reprod 2015; 30: 632-641.
[22] Zhang X, Shi H, Tang H, Fang Z, Wang J and Cui S. miR-218 inhibits the invasion and migration of colon cancer cells by targeting the PI3K/Akt/mTOR signaling pathway. Int J Mol Med 2015; 35: 1301-1308.
[23] Cao Y, Liu X, Lu W, Chen Y, Wu X, Li M, Wang XA, Zhang F, Jiang L, Zhang Y, Hu Y, Xiang S, Shu Y, Bao R, Li H, Wu W, Weng H, Yen Y and Liu Y. Fibronectin promotes cell proliferation and invasion through mTOR signaling pathway activation in gallbladder cancer. Cancer Lett 2015; 360: 141-150.
[24] Li Q, Shen L, Wang Z, Jiang HP and Liu LX. Tanshinone IIA protects against myocardial ischemia reperfusion injury by activating the PI3K/Akt/mTOR signaling pathway. Biomed Pharmacother 2016; 84: 106-114.
[25] Barra F, Ferro Desideri L and Ferrero S. Inhibition of PI3K/AKT/mTOR pathway for the treatment of endometriosis. Br J Pharmacol 2018; 175: 3626-3627.
[26] Choi J, Jo M, Lee E, Kim HJ and Choi D. Differential induction of autophagy by mTOR is associated with abnormal apoptosis in ovarian endometriotic cysts. Mol Hum Reprod 2014; 20: 309-317.
[27] Wang X, Yang B, She Y and Ye Y. The lncRNA TP73-AS1 promotes ovarian cancer cell proliferation and metastasis via modulation of MMP2 and MMP9. J Cell Biochem 2018; 119: 7790-7799.
[28] Farina P, Tabouret E, Lehmann P, Barrie M, Petrirena G, Campello C, Boucard C, Graillon T, Girard N and Chinot O. Relationship between magnetic resonance imaging characteristics and plasmatic levels of MMP2 and MMP9 in patients with recurrent high-grade gliomas treated by Bevacizumab and Irinotecan. J Neurooncol 2017; 132: 433-437.
[29] Li Y, Wang X, Wang X, Wan L, Liu Y, Shi Y, Zhang L, Fang Z and Wei Z. PDCD4 suppresses proliferation, migration, and invasion of endometrial cells by inhibiting autophagy and NF-kappaB/MMP2/MMP9 signal pathway. Biol Reprod 2018; 99: 360-372.
[30] Barisic A, Devic Pavlic S, Ostojic S and Pereza N. Matrix metalloproteinase and tissue inhibitors of metalloproteinases gene polymorphisms in disorders that influence fertility and pregnancy complications: a systematic review and meta-analysis. Gene 2018; 647: 48-60.